CORRESPONDENCE

Comments on "A Climatology of Cell Mergers with Supercells and Their Association with Mesocyclone Evolution" and "The Influence of Cell Mergers on Supercell Characteristics and Tornado Evolution on 27–28 April 2011"

JANNICK FISCHER,[a] MATTHEW D. FLOURNOY,[b,c,d] AND ANTHONY W. LYZA[d,e]

[a] Department Troposphere Research, Karlsruhe Institute of Technology, Karlsruhe, Germany
[b] NOAA/NWS/NCEP Storm Prediction Center, University of Oklahoma, Norman, Oklahoma
[c] School of Meteorology, University of Oklahoma, Norman, Oklahoma
[d] Cooperative Institute for Severe and High-Impact Weather Research and Operations, University of Oklahoma, Norman, Oklahoma
[e] NOAA/OAR/National Severe Storms Laboratory, Norman, Oklahoma

(Manuscript received 13 June 2023, in final form 26 July 2023, accepted 4 August 2023)

ABSTRACT: Two recent articles investigated the evolution of supercell mesocyclone intensity during storm merger events using radar-indicated azimuthal shear. Both found that initially strong mesocyclones tended to weaken while initially weak mesocyclones statistically most frequently tended to intensify during the merger. However, these studies did not include null cases. In this article, random supercell periods are analyzed to test if a similar pattern of mesocyclone intensity variations happens in the absence of mergers. A similar pattern is found, suggesting that these intensity variations are stochastic rather than linked to merger events. Based on this finding, the datasets and conclusions of the previous two articles are reevaluated collaboratively.

KEYWORDS: Mesoscale processes; Mesocyclones; Supercells; Tornadoes; Radars/Radar observations; Operational forecasting

1. Introduction

Two recent articles, Flournoy et al. (2022, hereafter F22) and Lyza and Flournoy (2023, hereafter LF23), have analyzed the evolution of supercell mesocyclone intensity during storm merger events. The main finding in both articles was that supercells with strong mesocyclones tended to weaken over the course of a cell merger while supercells with weak mesocyclones tended to intensify. Based on their data, the logical conclusion was that the cell merger was the direct cause for the mesocyclone strengthening or weakening. However, this implies that such mesocyclone intensity variations do not occur naturally, i.e., also in the absence of mergers. In fact, analysis of isolated supercell tornadoes in Fischer and Dahl (2023) indicated that nonmerger cases also show these intensity changes, but the dataset was relatively small. Hence, further analysis is necessary. This article tests the hypothesis of F22 and LF23 by analyzing mesocyclone intensity changes along *random* supercell tracks (section 2). Based on the results, the datasets of F22 and LF23 are reexamined (section 3). This comment article is based on discussions of the first author with the lead authors of F22 and LF23 (second and third author).

2. Random supercell periods in GridRad-severe

a. Methods

As in F22 and LF23, mesocyclone intensity is assessed by calculating WSR-88D radar azimuthal shear evolution along supercell tracks. The main difference here is that instead of analyzing merger events, random periods of random supercells were used. The tracks were taken from the 2010 and 2011 GridRad-Severe dataset (Murphy et al. 2023), which includes objectively defined storm tracks and their properties. To exclude nonsupercells, the five filter criteria of Homeyer et al. (2020) (their section 2d) were employed, which resulted in 4385 supercell cases (black tracks in Fig. 1). To keep computational expense to an acceptable level, only 7 days with intense supercell activity were selected for further analysis, including well-studied events such as 12 May 2010 (Markowski et al. 2018), 18 May 2010 (Skinner et al. 2014), and 24 May 2011 (Stratman and Brewster 2017). The rest of the methodology is mostly identical to F22 and briefly outlined below.

Although GridRad-Severe includes gridded radar data, azimuthal shear was taken from the MYRORSS database (Williams et al. 2022) to allow for direct comparability with F22 and LF23. Only the maximum low-level (0–3 km) azimuthal shear is presented here but the results using midlevel azimuthal shear (3–6 km) are qualitatively the same. Supercells that did not spend at least 30 min within 75 km of a radar location were excluded. Furthermore, 17 cases with obviously erroneous supercell classification (judging from radar reflectivity and velocity plots), wrong tracks, or missing MYRORSS data were filtered out manually. This resulted in 122 cases for the final analysis (red tracks in Fig. 1), comparable to the number of cases in F22 and LF23. Random 30-min periods[1] of each

Corresponding author: Jannick Fischer, jannick.fischer@kit.edu

[1] Periods of 20 and 25 min were also tested as well as averages between 20 and 30 min similar to LF23. The outcome was the same.

DOI: 10.1175/MWR-D-23-0120.1

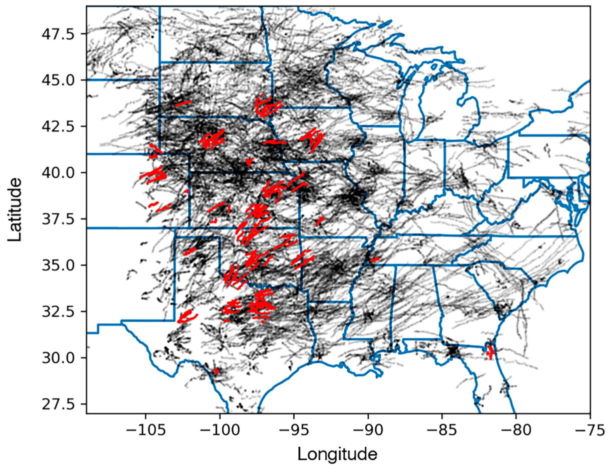

FIG. 1. Map of the initial 4385 supercells in 2010 and 2011 obtained from the GridRad-Severe dataset (black tracks) and the subset of 122 supercells for which MYRORSS azimuthal shear data were analyzed (red tracks). The latter occurred on 12 May 2010, 18 May 2010, 26 May 2010, 10 Jun 2010, 24 May 2011, 27 May 2011, and 20 Jun 2011.

supercell track were selected and for each MYRORSS time step the maximum azimuthal shear within a 10-km radius of the track was stored for the analysis below.

b. Results

Figure 2a shows the difference in azimuthal shear between the start and end of the 30-min period as a function of the starting value, comparable to Figs. 11 and 14a in F22 and LF23, respectively. *Despite the fact that random supercell periods were analyzed, the azimuthal shear change correlates negatively with the initial azimuthal shear.* The slope of the fitting line and the R^2 value are also in a similar range to F22 and LF23. To make this result more robust, the same analysis was performed using low-level azimuthal shear directly from the GridRad-Severe dataset[2] for all 4385 cases (black tracks in Fig. 1). The result is shown in Fig. 2b. It is clear that the same trend as in the MYRORSS data can also be seen in the GridRad-Severe data for a very robust number of cases. This suggests that during random 30-min supercell periods, weak mesocyclones tend to intensify while strong mesocyclones tend to weaken. This behavior is independent of merger events.

To explain this result, a red shading was added in Fig. 2. Pairs of values in this range cannot exist because a mesocyclone of a given intensity (e.g., 0.01 s^{-1} on the x axis) cannot weaken by more than this initial value (-0.01 s^{-1} on the y axis).[3] Hence, the values on the y axis stay way above the edge of the red area. No such range exists in the top-right corner of the plot because strong mesocyclones can theoretically always intensify. However, there is also a physical limit to mesocyclone intensity, so strong supercells statistically more often maintain their intensity or weaken. Likely for these reasons, the data points are concentrated from the top-left to the bottom-right areas of the plot, thereby causing a negative correlation. In other words, the main factor for the observed correlation seems that it is statistically more likely for a weak mesocyclone to intensify and vice versa.

3. Reanalysis of the F22 and LF23 datasets

In light of these findings, we reexamined azimuthal shear time series from the F22 supercell dataset. Figure 3 shows a scatterplot of initial azimuthal shear values versus the subsequent difference in azimuthal shear for random 30-min periods during each supercell's life cycle. Only one 30-min period from each storm's time series was included, yielding values for 321 of the 342 supercells in the dataset. The random selection of 30-min periods did not depend on merger/no-merger periods during each supercell's life cycle. As a result, some of the final 321 30-min periods in Fig. 3 contained mergers while others did not. The resulting R^2 value is less than those in Fig. 2a, but the best-fit line contains a slope and x intercept (around 0.01 s^{-1}) similar to those in Fig. 2a.

We also reexamined the dataset from 27 to 28 April 2011 detailed in LF23. We analyzed 92 independent 30-min periods during which no mergers were observed with the 29 tornadic supercells to evaluate mesocyclone intensity tendencies during periods without mergers and compare them to the tendencies detailed in Fig. 14 of LF23. Figure 4 summarizes the 30-min azimuthal shear changes observed for these independent, mergerless periods within the 27–28 April 2011 tornadic supercells, and Table 1 summarizes these statistics in comparison to the azimuthal shear change statistics surrounding individual merger, merger clusters, and the combination of all merger events in LF23. Overall, we note very little difference between the azimuthal shear tendencies as a function of initial azimuthal shear surrounding merger events and those within the 92 nonmerger periods analyzed.

4. Summary

This study tested the hypothesis of F22 and LF23 that merger events were often the direct cause for the strengthening of weak mesocyclones, as well as the weakening of strong mesocyclones. Analysis of randomly selected 30-min periods of GridRad-Severe supercell tracks do not support the hypothesis. Very similar mesocyclone intensity variations were observed during the random supercell tracks. Based on this result, the F22 and LF23 datasets were reexamined using random supercell periods instead of merger events, which yielded the same result. We conclude that mergers cannot indeed be statistically linked with mesocyclone intensity changes. In other words, mesocyclone intensity variations are at least partially a stochastic process. Weak mesocyclones often cannot weaken much further while still remaining supercellular, whereas strong mesocyclones simply are statistically more likely to weaken than intensify.

[2] Maximum azimuthal shear is available for all tracks in GridRad-Severe and, therefore, does not have to be explicitly computed unlike with the gridded MYRORSS data above.

[3] The maximum azimuthal shear is never negative (see Fig. 2) when only cyclonically rotating storms are considered.

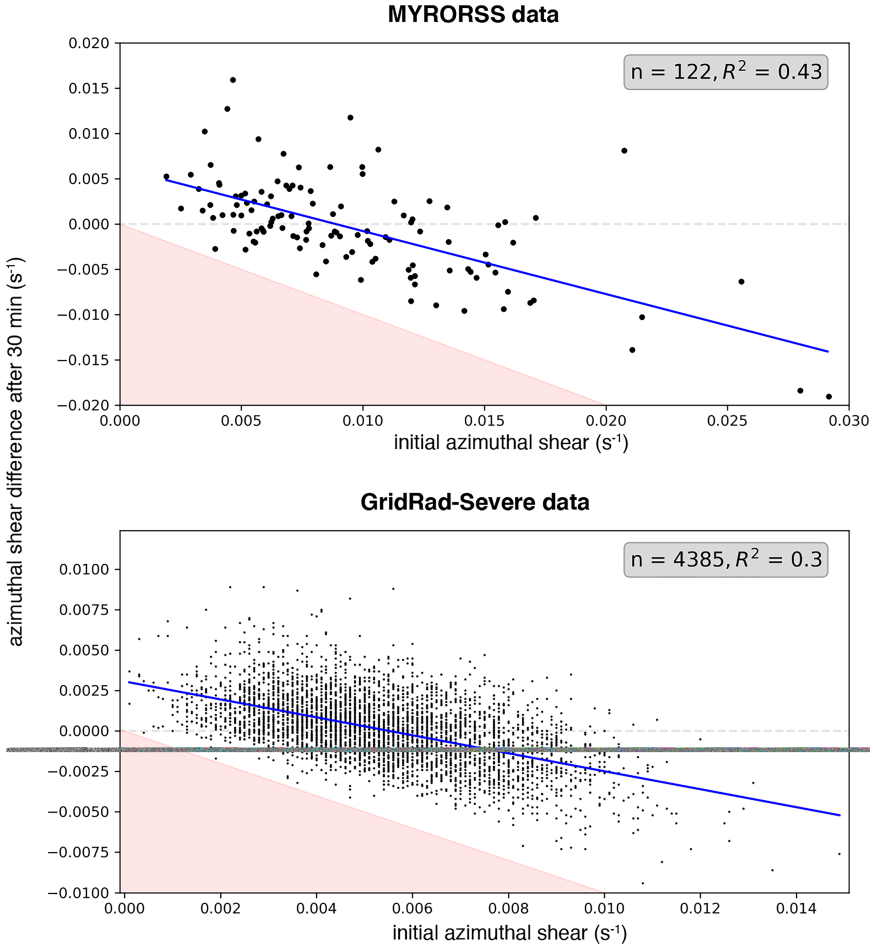

FIG. 2. Azimuthal shear change over 30 min as a function of the azimuthal shear value at the beginning of the period. (a) Each dot represents 1 of 122 supercells (red tracks in Fig. 1) during seven selected events. (b) Each dot represents 1 of the 4385 supercells (black tracks in Fig. 1) during 2010 and 2011. All tracks were obtained from the GridRad-Severe dataset as described in the text. Note that the axis range of azimuthal shear values differs because they were either determined from the MYRORSS [in (a)] or GridRad-Severe [in (b)] datasets and were hence subject to different processing procedures. The red shading represents an unphysical value range, as discussed in the text.

However, the four datasets (Figs. 2–4) yield very similar results, which gives confidence in the inverse relationship between initial mesocyclone strength and subsequent evolution of mesocyclone intensity. In other words, initially weaker mesocyclones tend to strengthen, and initially stronger mesocyclones tend to weaken. This potentially has important implications for real-time mesocyclone intensity prediction and we are currently working on a generalization of this relationship.

The conclusions herein do not question the importance of merger events for supercells and tornadoes in general. It is well established that such interactions *can* severely impact observed mesocyclone intensity (e.g., Flournoy et al. 2022; Fischer and Dahl 2023; Lyza and Flournoy 2023, and references therein). For instance, LF23 showed that tornado evolution was linked to merger occurrence, consistent with Lee et al. (2006). Ultimately, the relationships between tornadogenesis and tornado cessation and cell mergers may hold more promise for operational benefit than the relationship between mesocyclone intensity metrics and cell mergers, which appear masked behind the stochastic factors discussed in this study.

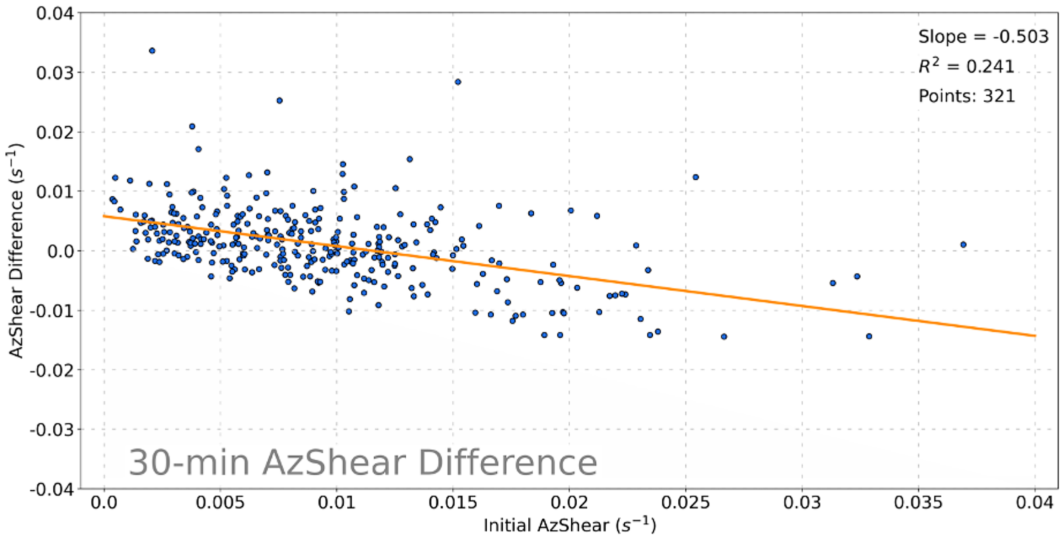

FIG. 3. Scatterplot of initial azimuthal shear values vs the subsequent 30-min difference in azimuthal shear for the F22 supercell dataset. The best-fit line is shown in orange, and the slope, R^2 value, and number of points (supercells) included in this plot are provided in the top-right corner.

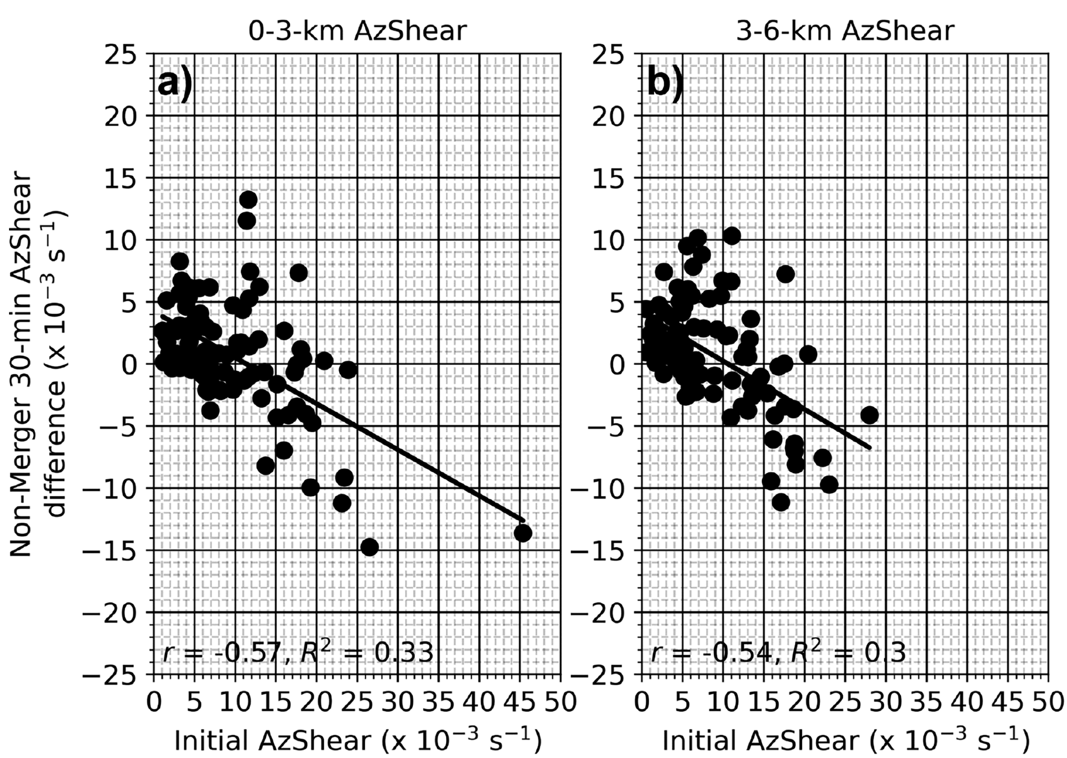

FIG. 4. Scatterplots of 30-min azimuthal shear change as a function of initial azimuthal shear value for (a) 0–3- and (b) 3–6-km azimuthal shear for the 92 independent no-merger periods analyzed within the life cycles of the 27–28 Apr 2011 tornadic supercells.

TABLE 1. Summary of slope, *y*-intercept, *x*-intercept, Pearson correlation coefficient (r), and coefficient of determination (R^2) statistics for the linear regression relationships between 30-min 0–3-/3–6-km azimuthal shear change as a function of initial azimuthal shear value for the merger periods detailed in LF23 (individual mergers, merger clusters, and combined individual mergers and clusters) as compared to the 92 independent no-merger periods analyzed in this study. All azimuthal shear, slope, *y*-intercept, and *x*-intercept values are expressed in units of 10^{-3} s^{-1}.

	Slope	*y* intercept	*x* intercept	r	R^2
Individual mergers	−0.441/−0.455	5.452/5.361	12.363/11.782	−0.42/−0.60	0.18/0.36
Merger clusters	−0.342/−0.583	4.422/6.989	12.930/11.988	−0.29/−0.55	0.08/0.31
Combined individual mergers and clusters	−0.366/−0535	4.723/6.293	12.904/11.763	−0.34/−0.57	0.11/0.32
No mergers	−0.371/−0.388	4.211/4.102	11.350/10.752	−0.57/−0.54	0.33/0.30

Acknowledgments. The authors thank Editor Chris Weiss and Editor-in-Chief Ron McTaggart-Cowan for their support of this collaborative comment article. Dr. Cameron Homeyer made this project possible by providing the GridRad-Severe dataset. Thanks are also extended to Dr. Michael Kunz and the Willis Research Network for allowing flexibility in the first author's research. Discussions with Drs. Johannes Dahl, Cameron Nixon, Alex Schueth, and Billy Faletti contributed to aspects of the study. This project was supported through NOAA/Office of Oceanic and Atmospheric Research under NOAA–University of Oklahoma Cooperative Agreement NA21OAR4320204, U.S. Department of Commerce. The statements, findings, conclusions, and recommendations are those of the authors and do not necessarily reflect the views of NOAA or the U.S. Department of Commerce.

Data availability statement. GridRad-Severe and MYRORSS data are available from Murphy et al. (2023) and Williams et al. (2022), respectively.

REFERENCES

Fischer, J., and J. M. L. Dahl, 2023: Supercell-external storms and boundaries acting as catalysts for tornadogenesis. *Mon. Wea. Rev.*, **151**, 23–38, https://doi.org/10.1175/MWR-D-22-0026.1.

Flournoy, M. D., A. W. Lyza, M. A. Satrio, M. R. Diedrichsen, M. C. Coniglio, and S. Waugh, 2022: A climatology of cell mergers with supercells and their association with mesocyclone evolution. *Mon. Wea. Rev.*, **150**, 451–461, https://doi.org/10.1175/MWR-D-21-0204.1.

Homeyer, C. R., T. N. Sandmael, C. K. Potvin, and A. M. Murphy, 2020: Distinguishing characteristics of tornadic and nontornadic supercell storms from composite mean analyses of radar observations. *Mon. Wea. Rev.*, **148**, 5015–5040, https://doi.org/10.1175/MWR-D-20-0136.1.

Lee, B. D., B. F. Jewett, and R. B. Wilhelmson, 2006: The 19 April 1996 Illinois tornado outbreak. Part II: Cell mergers and associated tornado incidence. *Wea. Forecasting*, **21**, 449–464, https://doi.org/10.1175/WAF943.1.

Lyza, A. W., and M. D. Flournoy, 2023: The influence of cell mergers on supercell characteristics and tornado evolution on 27–28 April 2011. *Mon. Wea. Rev.*, **151**, 1551–1569, https://doi.org/10.1175/MWR-D-22-0189.1.

Markowski, P. M., T. P. Hatlee, and Y. P. Richardson, 2018: Tornadogenesis in the 12 May 2010 supercell thunderstorm intercepted by VORTEX2 near Clinton, Oklahoma. *Mon. Wea. Rev.*, **146**, 3623–3650, https://doi.org/10.1175/MWR-D-18-0196.1.

Murphy, A. M., C. R. Homeyer, and K. Q. Allen, 2023: Development and investigation of GridRad-Severe, a multiyear severe event radar dataset. *Mon. Wea. Rev.*, https://doi.org/10.1175/MWR-D-23-0017.1, in press.

Skinner, P. S., C. C. Weiss, M. M. French, H. B. Bluestein, P. M. Markowski, and Y. P. Richardson, 2014: VORTEX2 observations of a low-level mesocyclone with multiple internal rear-flank downdraft momentum surges in the 18 May 2010 Dumas, Texas, supercell. *Mon. Wea. Rev.*, **142**, 2935–2960, https://doi.org/10.1175/MWR-D-13-00240.1.

Stratman, D. R., and K. A. Brewster, 2017: Sensitivities of 1-km forecasts of 24 May 2011 tornadic supercells to microphysics parameterizations. *Mon. Wea. Rev.*, **145**, 2697–2721, https://doi.org/10.1175/MWR-D-16-0282.1.

Williams, S. S., K. L. Ortega, and T. M. Smith, 2022: Multi-Year Reanalysis of Remotely Sensed Storms/MYRORSS_Data. OSF, accessed 6 March 2023, https://osf.io/9gzp2.